

On-chip radiation detection from stacked Josephson flux-flow oscillators

S. V. Shitov,^{a)} A. V. Ustinov,^{b)} N. Iosad,^{a)} and H. Kohlstedt

Institute of Thin Film and Ion Technology, Research Center (KFA), D-52425 Jülich, Germany

(Received 4 June 1996; accepted for publication 28 August 1996)

Radiation measurements with double-junction stacked Josephson flux-flow oscillator on-chip coupled to a superconductor–insulator–superconductor detector are reported. Impedance matching between the oscillator and the detector has been achieved using a broad band coupling circuit. Radiation power in the detector up to 10 nW has been measured in the frequency range between 170 and 410 GHz. Coherent radiation from two stacked junctions has been observed both at the fundamental Josephson frequency and at its second harmonic. The distribution of the radiation power between the first two harmonics allows us to distinguish between mutually coupled in-phase and out-of-phase flux-flow modes in the junctions. Coherent operation of stacked Josephson junction oscillators in the millimeter and sub-millimeter wave band is demonstrated. © 1996 American Institute of Physics. [S0021-8979(96)04723-8]

I. INTRODUCTION

Long Josephson junctions operated in the flux-flow mode, the so-called flux-flow oscillators (FFOs), recently showed very promising performance in integrated sub-millimeter wave band superconducting receivers.¹ Radiation from a FFO is induced by the motion of Josephson vortices, or fluxons, each of them carrying one magnetic flux quantum Φ_0 . In the integrated receiver design, the FFO operates as a local oscillator which pumps a small-area superconductor–insulator–superconductor (SIS) tunnel junction mixer placed on the same chip. Conventional single-barrier FFOs were proven to deliver a power of the order of $0.1\mu\text{W}$ at their first harmonic of radiation.^{2,3} Due to the losses in superconducting electrodes the maximum operation frequency of FFOs is limited by the frequency of about $f_\Delta = \Delta/(e\Phi_0)$ corresponding to the superconducting energy gap Δ , where e is the electron charge. Typically, for superconducting niobium the gap frequency f_Δ is in the range of 650–700 GHz. At the same time, the main receiver component such as SIS mixer can operate up to frequencies as high as $2f_\Delta$.⁴ Thus, extending the frequency limit of FFOs above f_Δ may substantially increase the presently available frequency range of integrated SIS receivers. On the other hand, increasing the maximum output power of FFOs may open new possibilities for off-chip applications in the future.

Vertical integration of several FFOs is a promising way to improve the oscillator performance. The mutual inductive coupling between the adjacent junctions in a stack is determined by the thicknesses of the superconducting layer(s) between the junctions and can be several orders of magnitude stronger than in case of their planar integration. Broad band tunable coherent operation of two stacked FFOs has been recently reported⁵ using dc measurements of their current–voltage characteristics (IVC). Due to the possibility of both in-phase and out-of-phase locking of fluxon oscillations in two stacked junctions,⁶ applications of stacked FFOs as

power multipliers and frequency doublers have been proposed.⁷

In this study, we report direct radiation detection experiments with stacked double-barrier Nb/(Al-AlO_x/Nb)₂ long Josephson junction FFOs using an SIS detector on the same chip. We observed two different mutually phase-locked modes of two junctions, the in phase and the out of phase. The radiation detected for the in-phase mode is characterized by high power at the fundamental harmonic of the single-barrier Josephson radiation frequency f_J , while the out-of-phase mode has shown the main emission at the second harmonic of f_J .

II. SAMPLES AND MICROWAVE CIRCUITRY

The goal of the design was to achieve a wide band coupling of a high-impedance small SIS tunnel junction with a distributed oscillator junction having an output impedance in the range of 0.3–0.6Ω. Two important demands have been taken into consideration. First, the coupling has to be wide band (at least one octave) to allow for detecting both the fundamental frequency of the oscillator and its second harmonic. Second, the device performance must be tolerant to certain parameter variations due to the fabrication process. The output impedance of a 6-μm-wide FFO stack has been estimated as the characteristic impedance of two Josephson transmission lines (JTLs) with their common electrode being of the same width as the top and bottom electrodes. The in-phase mode of the oscillator assumes that the microwave pulses are propagating in JTLs simultaneously as a single pulse of the same current but twice larger in voltage than for the single-layer JTL. This means that the output impedance of the stacked FFO is approximately twice larger than that of the single-layer FFO. In the case of out-of-phase mode, when the fluxon pulses in two JTLs are shifted by half of their period, the output impedance can be taken as equivalent to that of a single-layer FFO.

In order to be detected by the SIS junction with a typical impedance of 20–50 Ω, the FFO output radiation first has to be emitted into a micro-strip line with a characteristic impedance of about 10–20 Ω. For that purpose we used a three-

^{a)}Permanent address: Institute of Radio Engineering and Electronics, Russian Academy of Science, Mokhovaya St. 11, Moscow, 103907 Russia

^{b)}Electronic mail: a.ustinov@kfa-juelich.de

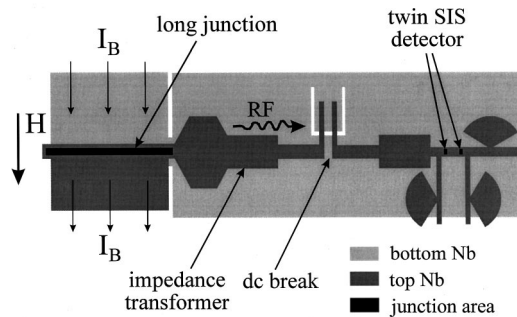


FIG. 1. Schematic top view of the device. The radiation from the stacked Josephson flux-flow oscillator (FFO) is coupled to the twin SIS detector via the strip-line impedance transformer ending in the dc break (dimensions are not to scale).

stage micro-strip impedance transformer (see Fig. 1) which provided 3 dB coupling within a frequency range of 140–480 GHz. To avoid the influence of discontinuities which occur at the corners of the transformer sections the latter have been tapered within 120°. The “tapered transformer” has been simulated using both numerical calculations and scale modelling which proved feasibility of this approach. The step-chain model for the tapered transitions⁸ was used for numerical analysis of these structures.

To avoid a dc electrical contact between the top electrodes of the FFO and the SIS detector, a dc block (dc break) as used in the original design⁹ has been incorporated into the transmission line connecting the FFO and the detector. The main idea of the dc block design is similar to the combination of two microwave baluns¹⁰ which are connected at the shortest possible distance to avoid an impedance discontinuity. The 3 dB bandpass of the dc block has been estimated as 100–500 GHz using both numerical simulations and scale model experiments.

The detecting cell was designed as a twin-junction structure^{11,12} employing two SIS junctions patterned in the same trilayer as the bottom layer FFO of the stack. The short micro-strip connecting the two junctions acts as a tuner of intrinsic capacitive impedance of the twin-junction cell. The two stage micro-strip impedance transformer is used for wide-band coupling of the incoming signal to the SIS detector. The exact transformer parameters have been calculated numerically and chosen to a certain extent empirically for the

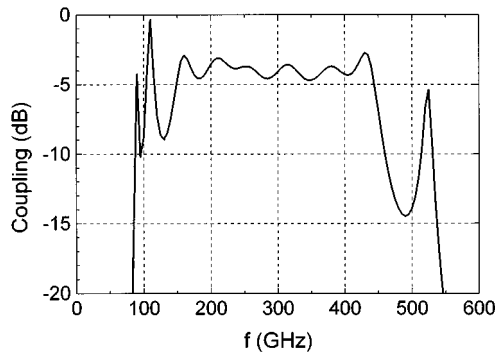


FIG. 2. The calculated overall frequency bandpass for the coupling circuit between the stacked FFO and the SIS detector.

reason of rather complicated interference of all components in the coupling circuit. The coupling is optimized at a nominal level of -6 dB and flatness 1 dB within the frequency range of 150–450 GHz, as illustrated by its calculated overall performance in Fig. 2.

The magnetic field for operating the FFO has been applied using an external solenoid. For suppressing the Shapiro steps in the SIS detector, we used the superconducting strip connecting the two SIS junctions as a local magnetic field control line (see Fig. 1). The leak of microwave power from the detector bias lines was blocked by low-pass filters formed by the radial stubs.

Several similar chips with various dimensions were fabricated on each wafer. Typically, a spread of the critical current density less than 5% has been achieved for two stacked tunnel barriers. In order to facilitate either the in-phase or the out-of-phase locking, we fabricated the wafers with two different thicknesses d of the intermediate Nb electrode between the tunnel barriers. These values $d=d_1=90$ nm and $d=d_2=140$ nm accounted for the coupling constants $S=S_1=-0.36$ and $S=S_2=-0.21$, respectively.¹³ In agreement with previous experiments,⁵ only the mutually out-of-phase locked regimes have been found stable for the intermediate coupling strength with $S=S_1$. For the weaker coupling with $S=S_2$, depending on the bias range, both in-phase and out-of-phase locking were successfully observed. In the following we present radiation detection data for a double-barrier 350- μ m-long and 6- μ m-wide FFO with $d=140$ nm. The used critical current density 950 A/cm² corresponded to the long junction limit with the single-barrier Josephson penetration depth $\lambda_J \approx 12$ μ m.

III. RESULTS

Fig. 3 presents stored traces of the FFO current–voltage (I – V) characteristics obtained in continuously varying magnetic field H . The flux-flow step is tunable in the broad voltage range up to 2.8 mV which is approximately twice as large as the single-barrier flux-flow range shown in Fig. 3 at higher

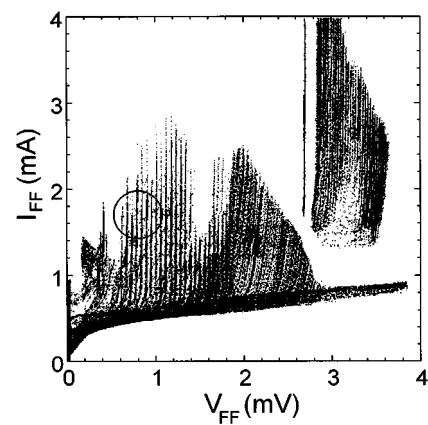


FIG. 3. Stored traces of I – V curves of the stacked oscillator obtained in continuously varying magnetic field H . The coherent double-junction flux-flow step is tunable in the voltage range between 0 and 2.8 mV. The circle indicates the voltage range at which the major radiation power has been detected.

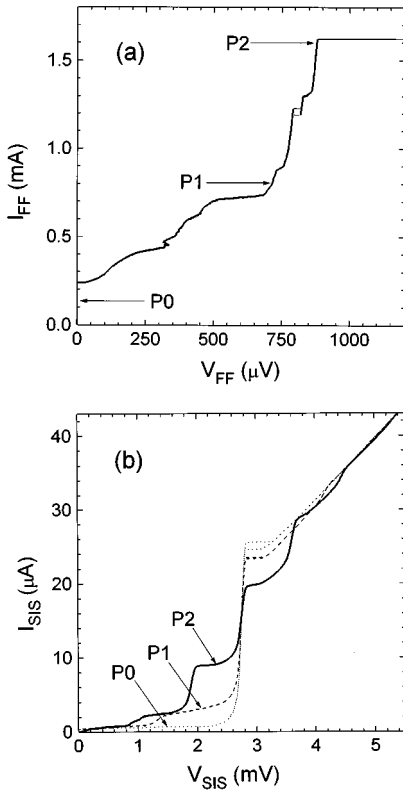


FIG. 4. (a) I – V characteristics of the double-junction stacked flux-flow oscillator in the magnetic field $H=7.7$ Oe. (b) I – V characteristics of the SIS detector corresponding to different bias points of the oscillator shown in Fig. 4(a): P0 (dotted line), P1 (dashed line), and P2 (solid line).

currents above the single-barrier gap $V_g=2.8$ mV. In the latter case, one of the junctions is switched to the gap voltage. Fig. 4(a) shows I – V characteristics in the applied magnetic field $H=7.7$ Oe where both stacked long junctions operate in the flux-flow regime. With increasing the bias current I_{FF} the voltage V_{FF} of the FFO approached its asymptotic value V_{FF}^H of about $880\text{ }\mu\text{V}$. At $I_{FF}=1.62\text{ mA}$ it switched to the double-barrier gap voltage at about 5.5 mV .

The detection of radiation from the stacked flux-flow oscillator is presented in Fig. 4(b). The I – V characteristics of the SIS detector correspond to different bias points (P0, P1, and P2) of the FFO shown in Fig. 4(a). The P0 curve accounts for the autonomous (not pumped) SIS characteristic. Under the influence of the radiation from the FFO, the photon-assisted tunnelling (PAT) steps are induced on the detector I – V curve around the gap voltage V_g (curves P1 and P2). The voltage width of the steps $\Delta V_{\text{PAT}}=hf/e$ is determined by the frequency f of the absorbed photons, where h is Plank's constant and e is the electron charge. For a single-barrier FFO biased at the voltage V_{FF} , the radiation frequency f is given by the Josephson relation $f=2\text{ eV}_{FF}/h$, and thus is proportional to V_{FF} . The first and rather striking observation from Fig. 4(b) is that the detected radiation frequency *decreases* with *increasing* the bias voltage V_{FF} from point P1 to point P2. In the following we show that this change occurs rather abruptly, and is due to the redistribution of the rf power between the first two harmonics.

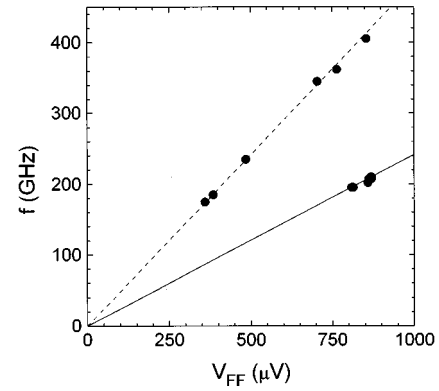


FIG. 5. The dominant radiation frequency detected by SIS twin junction as a function of the bias voltage V_{FF} of the stacked flux-flow oscillator along the I – V curve shown in Fig. 4(a). The expected first and second harmonics of the single-junction flux-flow voltages are shown by solid and dashed lines, respectively.

In order to accurately determine the radiation frequency and power, the pumped SIS detector I – V characteristics were analyzed quantitatively using Tucker's theory¹⁴ of SIS mixers. Fig. 5 shows the dependence of the dominant frequency detected by the SIS twin junction as a function of the bias voltage V_{FF} of the stacked FFO. Different points correspond to the radiation frequencies obtained from the analysis of the detector I – V curves measured for the different FFO bias points along the I – V curve shown in Fig. 4(a). The solid line and the dashed line correspond to the expected frequencies of the first and the second Josephson harmonics, respectively, calculated for the single-barrier FFO voltage $V_{FF}/2$. One can see that at low voltages (low fluxon velocities) the detected radiation corresponds to the second harmonic of the Josephson frequency $f_J=2\text{ eV}_{FF}/h$. At voltages $V_{FF}>800\text{ }\mu\text{V}$ (high fluxon velocities) the detected radiation corresponds to the first harmonic of f_J . This behavior is drastically different from the single-layer FFO where the power of the second and higher harmonics gradually increases with voltage.

The dependence of the radiation frequency on the flux-flow voltage V_{FF} is in a qualitative agreement with numerical simulations of flux-flow dynamics in two-barrier stacks.¹³ At low velocities fluxon chains simultaneously moving in two stacked junctions are locked out of phase, which corresponds to mutual repulsion between fluxons in neighboring junctions. In the resonant flux-flow regime the oscillation spectrum in each junction contains higher harmonics. The out-of-phase locking is characterized by a phase shift of π between two junctions which suppresses the total oscillation amplitude at the first harmonic. In contrast, the amplitude of the second harmonic is enhanced, which leads to the detection of the major frequency equal to $2f_J$ between $V_{FF}=350\text{ }\mu\text{V}$ and $V_{FF}=800\text{ }\mu\text{V}$. At high velocities fluxon chains in two junctions are phase locked in phase, which corresponds to mutual attraction between fluxons in two junctions. In our observations shown in Fig. 5 this corresponds to the main Josephson harmonic detected in the range of the stacked FFO voltage between $800\text{ }\mu\text{V}$ and $870\text{ }\mu\text{V}$. The emission of the first harmonic was found for two high velocity resonances at

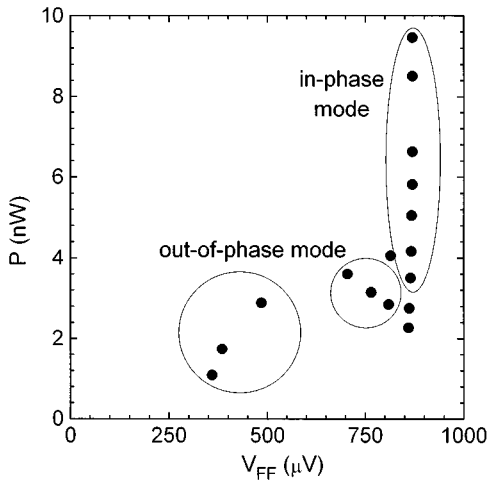


FIG. 6. Dependence of the detected radiation power (evaluated from pumped SIS detector $I-V$ curves) on the voltage V_{FF} of the stacked flux-flow oscillator along the $I-V$ curve shown in Fig. 4(a).

$I_{FF} > 1.2$ mA shown in Fig. 4(a). At the bottom of the highest resonance step the sharp transition from the second harmonic generation (observed at the very bottom of the step, at nearly constant bias voltage V_{FF}) to the first harmonic regime was clearly observed.

Finally, Fig. 6 presents the detected radiation power as a function of the voltage V_{FF} of the FFO. The absorbed power was evaluated from pumped SIS detector $I-V$ curves self-consistently with the frequencies reported in Fig. 5. Due to large normal resistance of the SIS detector $R_{SIS} \approx 120 \Omega$ (which corresponds to the actual junction area of about $1.8 \mu\text{m}^2$) a sufficiently high pumping level with well-pronounced PAT steps [see Fig. 4(b)] has been achieved already with the power of several nW. Fig. 6 shows a rapid increase of the power with increasing the bias current of the oscillator along the in-phase locked highest resonance step in Fig. 4(a). Such an efficient power enhancement is naturally expected for in-phase locked coherently operating FFOs, and might be of potential interest for applications. Using the same device in a similar bias current range, we also measured the radiation from the single-junction FFO (while another junction was switched to the gap state). We found the radiation power to be considerably lower (by factor of more than 4) than for the in-phase locked state of both junctions. Unfortunately, the power levels in these two cases cannot be compared directly because of the additional dissipative losses (produced by the quasi-particle injection in the middle superconducting film) which are due to the idle junction switched to the gap state.

IV. CONCLUSION

In summary, we reported the observation of millimeter-wave emission from mutually phase-locked modes in two-junction stacked Josephson flux-flow oscillators. The radiation detected in the in-phase mode is characterized by high power at the fundamental harmonic of the single-barrier Josephson radiation frequency f_J . The out-of-phase mode characterized by the dominant emission at the second harmonic of f_J might be feasible for the frequency doubling of the flux-flow oscillations. Since both the in-phase and the out-of-phase oscillation modes are expected also for stacks with large number of barriers,¹⁵ further studies in this direction appear to be promising for possible applications.

ACKNOWLEDGMENTS

This work was supported by the INTAS Grant No. 94-1783 and by the Russian Programme for Basic Research. The authors acknowledge fruitful discussions with V. P. Koshelets, E. Goldobin, and A. Wallraff.

- ¹V. P. Koshelets, S. V. Shitov, L. V. Filippenko, A. M. Baryshev, H. Golstein, T. de Graauw, W. Luinge, H. Schaeffer, and H. van de Stadt, *Appl. Phys. Lett.* **68**, 1273 (1996).
- ²V. P. Koshelets, A. V. Shchukin, S. V. Shitov, and L. V. Filippenko, *IEEE Trans. Appl. Supercond.* **3**, 2524 (1993).
- ³Y. M. Zhang, D. Winkler, and T. Claeson, *Appl. Phys. Lett.* **62**, 3195 (1993).
- ⁴W. C. Danchi and E. C. Sutton, *J. Appl. Phys.* **60**, 3967 (1986).
- ⁵A. V. Ustinov, H. Kohlstedt, and C. Heiden, *Appl. Phys. Lett.* **65**, 1457 (1994).
- ⁶A. V. Ustinov, H. Kohlstedt, and C. Heiden, *Physica C* **235-240**, 285 (1994).
- ⁷E. Goldobin, H. Kohlstedt, and A. V. Ustinov, *Appl. Phys. Lett.* **68**, 250 (1996).
- ⁸B. C. Wadell, *Transmission Line Design Handbook* (Artech House, 1991), pp. 306-307.
- ⁹S. V. Shitov, V. P. Koshelets, A. M. Baryshev, I. L. Lapitskaya, L. V. Filippenko, Th. de Graauw, H. Schaeffer, H. van de Stadt, and W. Luinge, *Proceedings of Sixth International Symposium on Space Terahertz Technology*, Pasadena, CA March 1995 (unpublished).
- ¹⁰V. Trifunovic and B. Jokanovic, *IEEE Trans. Microwave Theory Tech.* **42**, 1454 (1994).
- ¹¹V. Yu. Belitsky, S. W. Jacobsson, L. V. Filippenko, S. A. Kovtonjuk, V. P. Koshelets, and E. L. Kollberg, *Proceedings of the IV International Conference on Space Terahertz Technology*, Los Angeles, CA, 1993 (unpublished), p. 538.
- ¹²J. Zmuidzinas, H. G. LeDuc, J. A. Stern, and S. R. Cypher, *IEEE Trans. Microwave Theory Tech.* **42**, 698 (1994); J. Zmuidzinas, N. G. Ugras, D. Miller, M. Gaidis, H. G. LeDuc, and J. A. Stern, *IEEE Trans. Appl. Supercond.* **5**, 3053 (1995).
- ¹³A. Petraglia, A. V. Ustinov, N. F. Pedersen, and S. Sakai, *J. Appl. Phys.* **77**, 1171 (1995).
- ¹⁴J. R. Tucker and M. J. Feldman, *Rev. Mod. Phys.* **57**, 1055 (1985).
- ¹⁵R. Kleiner, *Phys. Rev. B* **50**, 6919 (1994).